Applied Catalysis B: Environmental 136–137 (2013) 150–159

Contents lists available at SciVerse ScienceDirect

Applied Catalysis B: Environmental

journal homepage: www.elsevier.com/locate/apcatb

A facile and efficient synthesis of styrene carbonate via cycloaddition of CO_2 to styrene oxide over ordered mesoporous MCM-41-Imi/Br catalyst

Jimmy Nelson Appaturi, Farook Adam *

School of Chemical Sciences, Universiti Sains Malaysia, 11800 Penang, Malaysia

ARTICLE INFO

Article history:
Received 22 April 2012
Received in revised form 4 January 2013
Accepted 29 January 2013
Available online 7 February 2013

Keywords:
Cycloaddition
Styrene oxide
Styrene carbonate
Carbon dioxide
Imidazole

ABSTRACT

MCM-41 was successfully immobilized with imidazole using 3-chloropropyltriethoxysilane (CPTES) as the anchoring agent followed by alkylation with 1,2-dibromoethane at 110 °C. The resulting catalyst was designated as MCM-41-Imi/Br. TEM showed the catalyst had ordered mesoporous straight-channels with average wall thickness of 2.14 nm and average pore size of 1.56 nm. The ^{29}Si MAS NMR analysis confirmed the presence of T^2, T^3, Q^3 and Q^4 silicon centers. The ^{13}C MAS NMR showed that MCM-41-Imi/Br had three chemical shifts corresponding to the three carbon atoms of the propyl group. The aromatic imidazole peaks were detected at 110–140 ppm. The catalyst was used in the solvent-less synthesis of styrene carbonate (SC) from CO_2 and styrene oxide (SO) under ambient conditions. It was demonstrated that the synergistic effect due to the stronger nucleophilicity of Br^- and amine in the catalyst could lead to a maximum selectivity of 99.1%. Based on the results, a plausible reaction mechanism was proposed for the catalytic reaction. The catalyst could be recovered and reused several times without significant loss in the catalytic activity.

1. Introduction

Naturally, the presence of carbon dioxide (CO_2) in the atmosphere is to help in the photosynthesis of plants for their food. Even though this gas has a pivotal role for all the living things in the world, it is also the main constituent among the greenhouse gases [1]. About 32% of CO_2 is produced due to hydrocarbon combustion and gasification and are being released into the atmosphere. The use of fossil fuel in transportation releases ~30% of the total CO_2. The natural phenomena such as volcanic eruption and decay of plants and animals also release CO_2 into the atmosphere. As a consequence, the CO_2 concentration increased in the atmosphere and has resulted in severe climatic change due to the greenhouse effect [2]. In recent years, various utilization of this naturally abundant CO_2 has gained considerable momentum in an effort to reduce the concentration of CO_2 in the atmosphere.

Carbon dioxide is a linear molecule with double bonds between the carbon and oxygen atoms (O=C=O). It is a colourless and odourless gas. It is recognized as a non-flammable, non-toxic, inexpensive reagent and environmentally benign molecule [3]. It is a safe, renewable carbon source [4] and thermodynamically stable compound [5]. It is a kinetically inert molecule and is used as C1 building block in organic synthesis [6]. More importantly it is a substitute for the poisonous and toxic phosgene, carbon monoxide and isocyanates [1] in chemical reactions. Carbon dioxide plays a versatile role in the process of various chemical transformations such as in the production of formic acid, dialkyl carbonate, dimethyl formamide, methanol, urea, salicylic acid, cyclic carbonates, and polycarbonates. Apart from this, the cycloaddition of CO_2 with epoxide has attracted much attention lately [7].

Since 1967, the production of cyclic carbonate from the cycloaddition reaction is well established [8]. These cyclic carbonate compounds are colourless, odourless and biodegradable [9]. They are widely used as aprotic polar solvents, additives and also monomers for polymer synthesis [7]. Besides, it has been used in electrolytic materials such as secondary batteries (lithium batteries), resins, cleaning, cosmetics and personal care products [10]. Furthermore, cyclic carbonates are used as intermediates for pharmaceutical and biomedical fine chemical synthesis [4]. In the agricultural industry, cyclic carbonates are used in the synthesis of herbicides and disinfectants [11]. In addition, cyclic carbonates also play an important role as an intermediate for the synthesis of fuel additives [12].

Recently, a wide range of homogeneous and heterogeneous catalysts have been developed to catalyze the reaction for the generation of cyclic carbonates. Both homogeneous and heterogeneous catalysts have their own advantages and disadvantages. Usually,

* Corresponding author. Tel.: +60 46533567; fax: +60 46574854.
E-mail addresses: farook_dr@yahoo.com, farook@usm.my, farookdr@gmail.com (F. Adam).

0926-3373/$ – see front matter © 2013 Elsevier B.V. All rights reserved.
http://dx.doi.org/10.1016/j.apcatb.2013.01.049

homogeneous catalyst give higher catalytic activity compared to heterogeneous catalysts. Heterogeneous catalysts have the inherent problem of lower activity and need the use of co-solvent [9]. However, homogeneous catalysts are undesirable in industry due to the catalyst-product separation problem [13] which may require more energy and may result in the decomposition of the catalysts [4]. Therefore, heterogeneous catalysts are more suitable for the continuous flow operation and it is more appropriate than batch wise process for large scale industrial synthesis [5]. Besides, it can also be easily separated from the reaction products [2] and be subjected for regeneration for subsequent reuse. However, due to the lower activity, it is important to design and synthesize more efficient heterogeneous catalysts. The production of cyclic carbonates like all other chemical synthesis, not only depends on the type of catalyst, but also other reaction conditions such as reaction time, temperature, pressure and the type of solvent.

Rice is a primary source of food for billions of people and its cultivation covers 1% of the earth's surface. In Malaysia, approximately 163000 MT (1.24%) of rice has been produced and about 0.575 MT of rice husk was generated in 2011 [14]. Rice husk is an agricultural residue (biomass), produced from the processing of rice and is either burnt or dumped as waste. The ash is composed of 92–95% silica (SiO_2). It is highly porous and lightweight, with a very high external surface area [15]. Such attributes of materials can be taken advantage of to synthesize value added materials from this biomass.

In this current study, imidazole (Imi) was immobilized on MCM-41 using a 3-step process to give MCM-41-Imi/Br. This catalyst was successfully used for the synthesis of styrene carbonate (SC). The influence of various experimental factors such as temperature, CO_2 pressure, catalyst amount, reaction time and effect of reaction medium forms the basis of discussion reported in this communication. To the best of our knowledge this is the first report on the utilization of rice husk ash (RHA) as a support for the cycloaddition of CO_2 to styrene oxide (SO).

2. Experimental

2.1. Raw materials

The rice husk (RH) was obtained from a rice mill in Penang. Other materials used were silica gel (70–230 mesh, Merck), nitric acid (QRec, 65%), sodium hydroxide pellets (R&M Chemicals, 99%), acetone (Qrec, 99.5%), cetyltrimethylammonium bromide (CTAB) (Riedel-de Haen, 98%), 3-chloropropyltriethoxysilane (CPTES) (Sigma–Aldrich, 95%), toluene (Qrec, 99.5%), acetonitrile (Qrec, 99.5%), *N*,*N*-dimethylformamide (Qrec, 99.8%), 1,2-dichloroethane (Fisher Scientific, 99.9%), styrene oxide (SΛFC, > 97%), 1,2-dibromoethane (Merck, > 99%) and imidazole (Scharlau, 99%). The carbon dioxide was purchased from CAMBREX-HENKEL, Pinang and used as received. Other reagents used were of analytical grade and used without further purification.

2.2. Catalyst preparation

2.2.1. Preparation of MCM-41

MCM-41 was prepared according to the method of Appaturi et al. [16], using RHA as a silica source and CTAB as template. The resulting gel was aged at 80 °C for 48 h. The gel was separated by centrifugation and vacuum filtration and then washed with distilled water followed by acetone. The solid obtained was dried at 100 °C for 24 h, ground in a mortar and calcined in a muffle furnace at 600 °C for 6 h.

2.2.2. Preparation of Cl-MCM-41

To prepare Cl-MCM-41, 4.0 mL (16.6 mmol) of CPTES was added slowly into a mixture of 2.0 g of MCM-41 and 30 mL of dry toluene. The reaction mixture was refluxed at 110 °C in a temperature controlled oil bath. After 24 h of refluxing, the flask was cooled to room temperature. The solid phase was filtered and washed twice with dry toluene, once with ethanol and distilled water to remove the un-reacted CPTES. The solid sample was then dried at 100 °C for 24 h and ground with a mortar and pestle to afford the Cl-MCM-41.

2.2.3. Synthesis of MCM-41-Imi

Imidazole (1.13 g, 16.6 mmol) was added to a suspension containing Cl-MCM-41 (2.0 g), dry toluene (30 mL) and triethylamine (Et_3N) (2.3 mL, 16.6 mmol). The mixture was refluxed at 110 °C for 24 h. The solid sample was separated by filtration and washed twice with dry toluene and thrice with ethanol to remove the excess amount of imidazole. After drying at 100 °C for 24 h, the sample was ground to fine powder and labeled as MCM-41-Imi.

2.2.4. Synthesis of MCM-41-Imi/Br

To prepare MCM-41-Imi/Br, 2.0 g of MCM-41-Imi was added into 30 mL of dry toluene. 1,2-dibromoethane (1.4 mL, 16.6 mmol) was added slowly and the mixture was refluxed at 110 °C for 24 h. The excess alkyl halide was removed by filtration, followed by repeated washing with dichloromethane. The resulting solid was then dried in an oven at 100 °C for one day. The reaction sequence and the possible structure of MCM-41-Imi/Br is shown in Scheme 1.

2.3. Catalyst characterization

The powder X-ray diffraction patterns of the catalyst were recorded on a Siemens X-ray powder diffractometer (D5000, Kristalloflex) equipped with Cu Kα radiation (λ = 0.15406 nm). The Bruner–Emmett–Teller (BET) and Barrett–Joyner–Halenda (BJH) parameters were obtained from N_2-sorption analysis using a porosimeter (model NOVA Quantachrome porosimeter 2000e) at −196 °C. The surface morphology and topography images were obtained with a transmission electron microscope (TEM), model Phillips CM12, and scanning electron microscope (SEM), model Leica Cambridge S360 respectively. The elemental analysis was carried out using energy-dispersive X-ray spectroscopy (EDX Falcon System) and CHN analyses were carried out using PerkinElmer Series II, 2400. The FT-IR spectra were obtained using PerkinElmer System 2000. The ^{29}Si and ^{13}C Magic Angle Spinning Nuclear Magnetic Resonance (MAS NMR) was recorded using solid-state NMR instrument (400 MHz Bruker AVANCE III). Thermogravimetric analysis (TGA) was performed using (TGA SDTA851^e) Mettler Toledo equipment.

To study the active sites for CO_2 activation, the MCM-41-Imi/Br (300 mg) was heated to 140 °C and exposed to CO_2 for 2 h. The FT-IR spectra of the samples were recorded before and after exposure to CO_2 using PerkinElmer System 2000.

In order to confirm the exact amount of bromide in the catalyst, ion chromatography (IC) analyses was carried out. A 100 mg of MCM-41-Imi/Br was dissolved in 25 mL of 1 mol/L sodium hydroxide. The solution was stirred for 24 h. A clear solution was obtained after filtration with 0.45 μm Nylon Milipore filter. About 2 mL of the solution was transferred into 100 mL volumetric flask and made up with deionized water. The analysis was conducted on IC equipment (Model: Metrohm 792 Basic IC), with anion column, METROSEP ASUPP 5–150, (size: 150 mm × 4.0, particle size: 5.0 μm), conductivity detector and ICNet 2.3 computer software for data handling to determine the presence of bromide. The mobile phases were 1.0 mmol L^{-1} sodium carbonate with 3.2 mmol L^{-1} sodium bicarbonate as first eluent and 100 mmol L^{-1} of sulphuric acid as second eluent. The flow rate was 0.70 mL min^{-1}, and the injection volume was 1 mL.

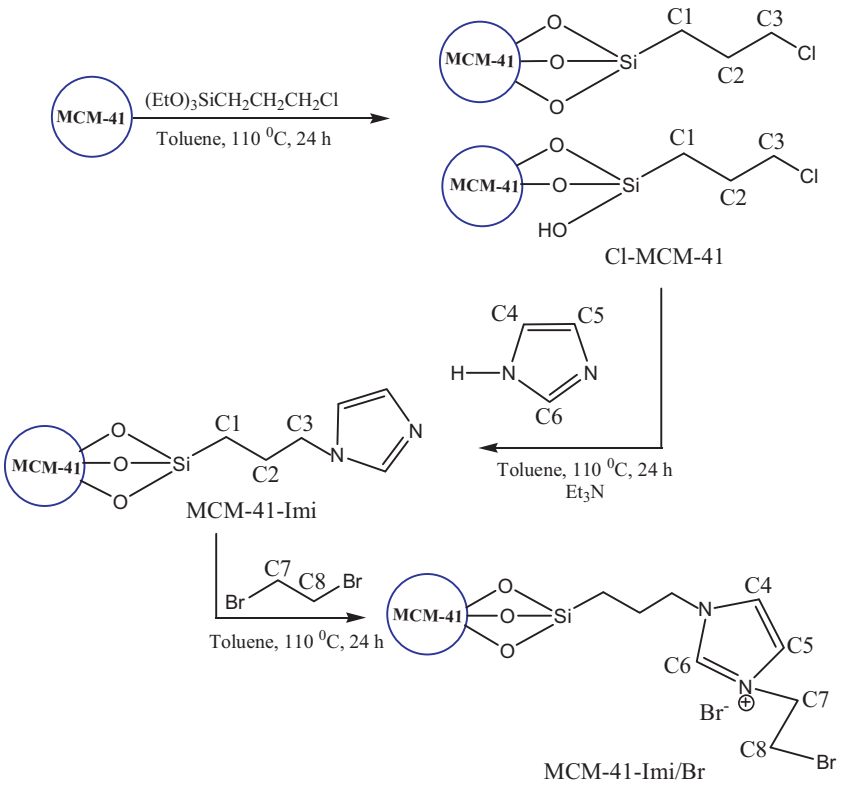

Scheme 1. The reaction sequence and the possible structure for MCM-41-Imi/Br.

2.4. Cycloaddition reaction

In a typical catalytic reaction, styrene oxide (30 mmol), 50 mL of acetonitrile as solvent and 300 mg of activated catalyst were charged into a high pressure laboratory autoclave (Carl Roth, Germany) equipped with a magnetic stirrer and heating mantle system. After being sealed, the reactor was carefully flushed once with CO_2. About 40 bar of CO_2 was dosed into the reactor and heating and stirring were started. After having reached the working temperature (140 °C), the reaction was allowed to proceed for 10 h. After the reaction was completed, the autoclave was allowed to cool down to room temperature, and the excess CO_2 was released by opening the outlet valve. After depressurization, the autoclave was opened slowly and the reaction mixture was separated by filtration.

To a 0.5 mL of the reaction product, 20 μL of cyclohexanol was added as the internal standard. The resulting mixture was analyzed by gas chromatography (Clarus 500 PerkinElmer) equipped with an Elite Wax, capillary column (PerkinElmer) (30 m length, 0.32 mm inner diameter and 0.25 μm film thickness) and a flame ionization detector (FID); with nitrogen as carrier gas. The temperature program used for the analysis were: initial oven temperature 100 °C; ramp 1:at 30 °C min^{-1} for 2.3 min, followed by ramp 2: at 30 °C min^{-1} for 2 min, then hold for 4 min; injector port temperature: 250 °C; detector temperature: 250 °C. A reaction mixture were also analysed by GC–MS (Clarus 600 PerkinElmer) with a mass selective detector and helium as the carrier gas to further identify the formation of product and side product. After the reaction was complete, the product was concentrated and purified by column chromatography with 20% hexane in chloroform as the eluting solvent. A purified fraction was then analysed by FT-IR (PerkinElmer system 2000), GC–MS (Clarus 600 PerkinElmer) followed by ^{1}H NMR (500 MHz Bruker AVANCE III).

3. Results and discussion

3.1. Catalyst characterization

The low-angle powder XRD pattern of MCM-41 and its immobilized derivatives are shown in Fig. 1. The reflection at 2.5° (1 0 0) plane on the 2θ axis is the characteristic peak of the 2D hexagonal (*p6mm*) space group which was later proved by the TEM images. The presence of peaks corresponding to the (1 1 0) and (2 0 0) planes clearly show the presence of highly ordered mesopores with well defined pore structure [16]. It clearly shows that the host material has a high intensity of (1 0 0) plane compared with the immobilized catalyst. This shows that the immobilization process had affected the pore structure. The TEM (Fig. 2) results clearly reveal the presence of ordered arrays of mesopores with

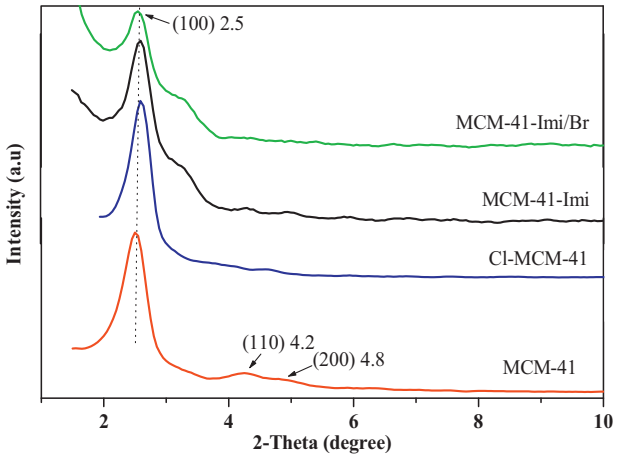

Fig. 1. The low-angle XRD patterns of modified MCM-41 materials.

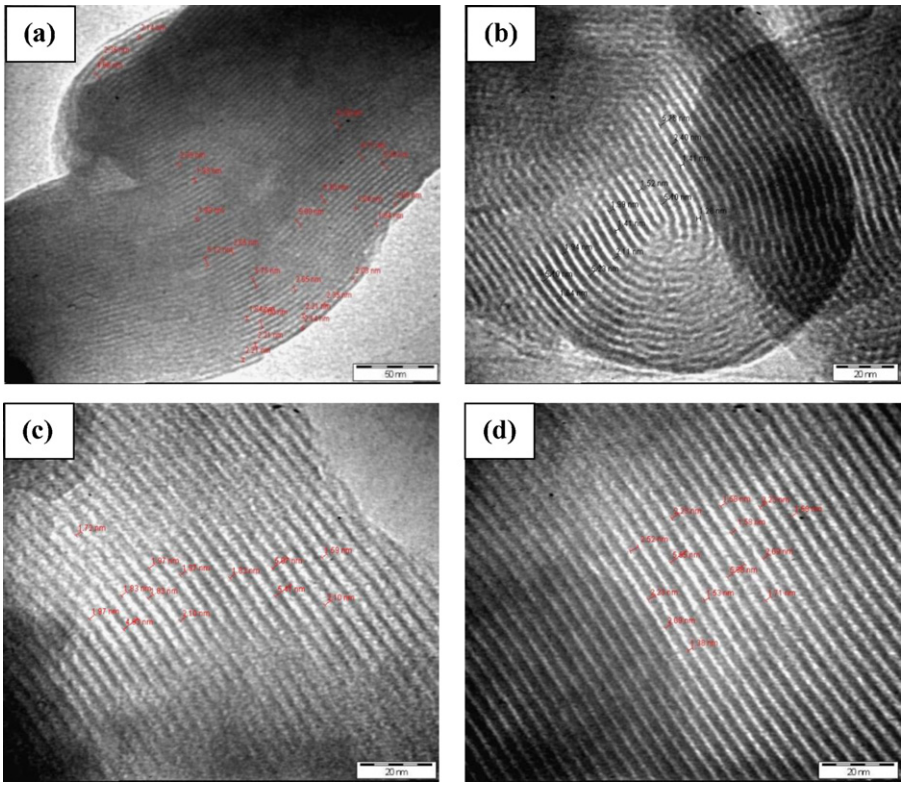

Fig. 2. The TEM micrographs of (a) MCM-41 at ×240 K, (b) Cl-MCM-41, (c) MCM-41-Imi and (d) MCM-41-Imi/Br at ×550 K.

uniform pore size and wall thickness for all the prepared samples. However, there is a slight difference in the value of pore size and wall thickness estimated from TEM. In Cl-MCM-41 (Fig. 2(b)) it was found that the mesopores formed curved pores. It has been known that hexagonally ordered mesopores could be curved under some synthetic conditions. Thus, we believe that the properties of the added CPTES species might affect the morphology of the material. The added CPTES may coordinate with oxygen or hydroxyl groups of the silicate seeds, affecting the van der Walls' attractive force and electrical double layer repulsive interactions between the colloidal seeds and silicate micelles. This causes the generation of end-to-end (homeotropic anchoring) growth resulting in pore curvature [17]. The SEM results for MCM-41 showed micellar rod-like shape or spherical edges. This could be due to the CTAB surfactant molecules assembled directly into hexagonal structure upon addition to the silicate species. However these initial shapes slowly agglomerate after the immobilization process as shown in other SEM images in Supplementary Figure 1.

Table 1 shows the derived parameters from the XRD and the BET analysis. The BET results show a reduction in surface area from 1115 m^2g^{-1} for MCM-41 to 585 m^2g^{-1} for Cl-MCM-41 and 302 m^2g^{-1} and 130 m^2g^{-1} for MCM-41-Imi and MCM-41-Imi/Br respectively. This reduction in the specific surface area is due to the immobilization of the organic moieties. The pore size was calculated using the BJH method. The pore size was also found to be much smaller in the MCM-41-Imi/Br compared to the parent MCM-41. This is due to the pore blockage by the immobilized ligand.

Fig. 3 shows the FT-IR spectra of the host and grafted materials. The prepared materials show a broad vibration band in the range of 3000–3500 cm^{-1} attributed to the O—H of hydrogen bonds in SiO—H and the HO—H of water molecules adsorbed on the catalyst surface. The band at 964 cm^{-1} corresponds to the symmetric stretching vibration of Si—OH. The band at 1634 cm^{-1} is due to the bending vibration from H_2O which was trapped in the silica framework. The band at 1096 cm^{-1} is attributed to the asymmetric Si—O—Si stretching vibration [18]. The bands at 802 cm^{-1}, and 470 cm^{-1} are due to the bending and vibration modes of Si—O—Si respectively [19]. The imidazole ring is identified by the appearance of the N—H vibration band at 3468–3416 cm^{-1}. However, these bands are embedded within the broad bands due to the OH vibrations. The bands observed in the range of 2800–3000 cm^{-1} were assigned to alkyl C—H stretching bands. The band at 1619 cm^{-1} is due to conjugated C=N vibration of the cyclic system (imidazole) which is clearly shown in the cut-out of the IR spectra [20]. A week signal at 625 cm^{-1} (C—Br) demonstrated the fuctionalization of MCM-41-Imi with 1,2-dibromoethane. All the vibration bands indicates the successful anchorage of imidazole and 1,2-dibromoethane.

Table 1
The textural properties of the prepared materials.

Catalyst	Surface area[a] ($m^2\,g^{-1}$)	Pore size[a] (nm)	Pore volume[a] ($cm^3\,g^{-1}$)	Unit cell parameter[b] (nm)	d_{100}[b] (nm)	Pore wall thickness[c] (nm)
RHA	273	3.6	0.34	–	–	–
MCM-41	1115	2.3	0.92	4.17	3.63	1.85
Cl-MCM-41	585	2.3	0.55	4.71	4.08	2.39
MCM-41-Imi	302	1.3	0.30	3.92	3.40	2.66
MCM-41 Imi/Br	130	1.2	0.18	4.08	3.53	2.84

[a] Values obtained from N_2 sorption studies.
[b] Values obtained from XRD studies.
[c] Pore wall thickness = unit cell parameter–pore size.

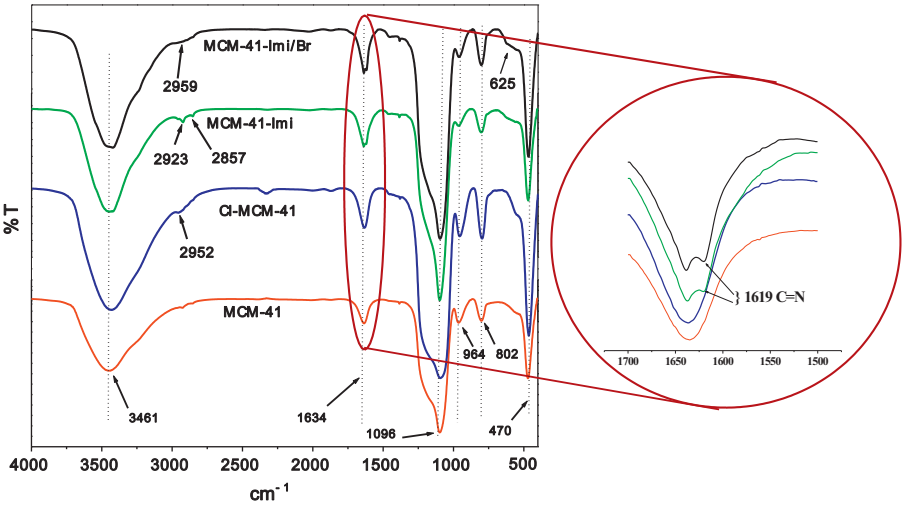

Fig. 3. The FT-IR spectra of MCM-41, Cl-MCM-41, MCM-41-Imi and MCM-41-Imi/Br. The magnified graph shows the expansion of the FT-IR spectra of all the catalysts in the region of 1700–1500 cm^{-1}.

The results of elemental and ion chromatography analyses are listed in Table 2. The CHN analysis showed about 4.46% of carbon and 0.87% of hydrogen present in Cl-MCM-41. This composition was much higher in MCM-41-Imi in which 9.32% of carbon and 1.58% of hydrogen and 2.54% of nitrogen were detected. The carbon content was even higher in MCM-41-Imi/Br (9.66%) as expected in comparison to MCM-41-Imi. From the EDX analysis the amount of Cl present in Cl-MCM-41 was 0.76%. Furthermore, MCM-41-Imi/Br showed the presence of nitrogen (5.80%) and bromine (2.72%) respectively. The amount of bromide per gram of MCM-41-Imi/Br was calculated based on the IC result. The concentration of bromide in MCM-41-Imi/Br was found to be 0.44 mmol/g. The percentage loading and surface coverage of organic moieties on per gram of silica was calculated based on the reported literature [21] and it was found to be 47.78% and 2.77 μ mol m^{-2} respectively. These results confirmed the immobilization of imidazole and 1,2-dibromoethane on the silica.

The organic content of the grafted silica was determined by thermogravimetric analysis (TGA). The results are depicted in Supplementary Figure 2. The TGA of all the prepared material showed water loss between 30–140 °C at the first stage. The second mass loss occurred between 137 and 394 °C (ca. 32.46%, 3.2461 mg) indicates the removal of CTAB from MCM-41 (before calcination). The third mass loss (ca. 9.73%, 0.9727 mg) observed between 311 and 522 °C was attributed to the decomposition of CPTES in Cl-MCM-41[20]. 1,2-dibromoethane and imidazole was decomposed at 135–296 °C (ca. 2.87%, 0.3019 mg) and 296–414 °C (ca. 2.00%, 0.2104 mg) respectively in MCM-41-Imi/Br. The final mass loss around 400–900 °C observed in all the materials indicates the loss of water during the condensation of silanol groups.

The ^{13}C MAS NMR of Cl-MCM-41 (Fig. 4) showed peaks at 7.4 (C1), 24.0 (C2) and 44.0 (C3) ppm, corresponding to the carbon atoms shown in Scheme 1. In MCM-41-Imi, the chemical shifts for the propyl carbons were shifted to down field compared to that observed in Cl-MCM-41. This was attributed to the immobilization of the imidazole. The presence of the aromatic imidazole could be observed in the region of 110–140 ppm. The *cis* carbons of imidazole (C4 and C5) were observed as a shoulder at 121.0 and 119.2 ppm. However, there was not much shift in the peak for MCM-41-Imi/Br compared to MCM-41-Imi. The peaks for C7 and C8 corresponding to 1,2-dibromoethane are not seen as it may be overlapping with the other alkyl carbon signals.

The solid state ^{29}Si MAS NMR analyses for all the prepared materials were also carried out (not shown). MCM-41 showed distinctive peaks at −109, −101 and −91 ppm corresponding to Q^4 ($Si(OSi)_4$), Q^3($Si(OSi)_3(OH)$) and Q^2 ($Si(OSi)_2(OH)_2$) silicon atoms respectively. However, the Q^2 peak disappeared in MCM-41-Imi and MCM-41-Imi/Br due to the immobilization of organic moieties compared to MCM-41 and Cl-MCM-41. The Cl-MCM-41 showed T^2 (−57.3 ppm) and T^3 (−66.0 ppm) peaks which further confirmed the presence of organosiloxane units. These peaks shifted down field in MCM-41-Imi: T^2at −58.0 ppm, T^3at −67.2 ppm, and in MCM-41-Imi/Br: T^2 at −63.0 ppm, T^3 at −72.2 ppm. This is due to the electron withdrawing effect of the added bromine in MCM-41-Imi/Br. The shifting of the peaks further confirmed the successful immobilization of organic ligand. A similar change was observed by Udayakumar et al. [22].

Table 2
Elemental and ion chromatography analyses of the catalysts.

Entry	Catalyst	Elemental analysis (wt.%)			Amount of organic amine (mmol/g)[a]	Amount of bromide ion (mmol/g)[b]
		C	H	N		
1	MCM-41 (before calcination)	40.50	4.65	1.29	0.92	0.38[c]
2	MCM-41 (after calcination)	0.13	2.00	–	–	–
3	Cl-MCM-41	4.46	0.87	–	–	–
4	MCM-41-Imi	9.32	1.58	2.54	0.91	–
5	MCM-41-Imi/Br	9.66	1.56	2.87	1.03	0.44

[a] Calculated based on amount of nitrogen from elemental analysis.
[b] Calculated based on ion chromatography analysis.
[c] The value is obtained due to the presence of CTAB in the catalyst.

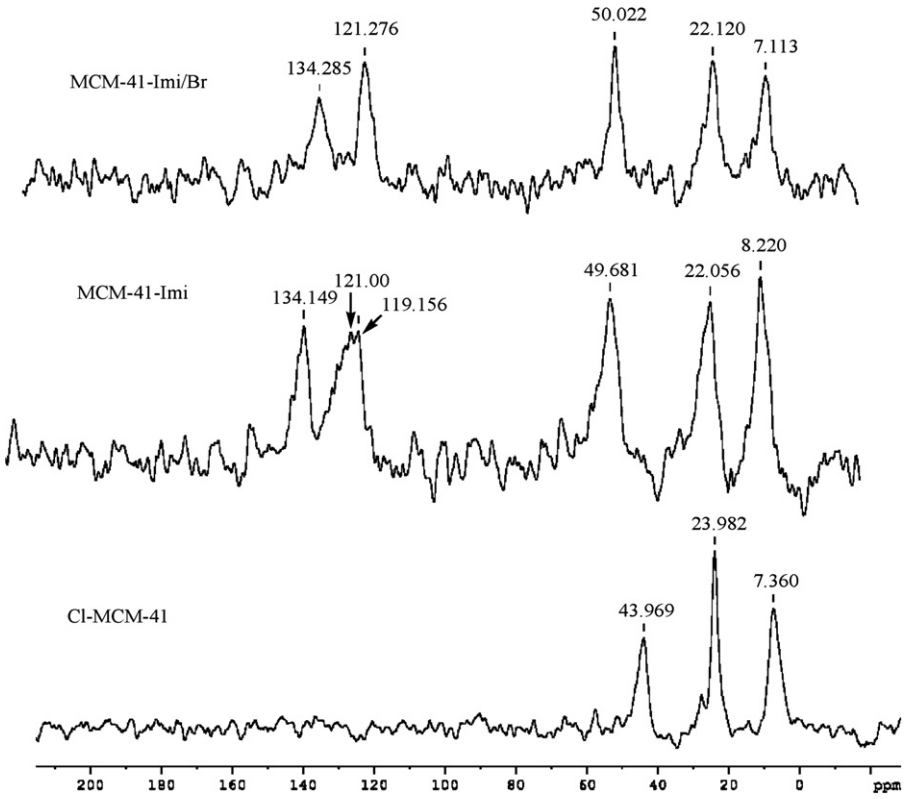

Fig. 4. The ^{13}C MAS NMR spectra for all the prepared materials.

3.2. Catalytic activity

3.2.1. Synthesis of styrene carbonate

The effect of various catalysts on the cycloaddition of carbon dioxide and styrene oxide was investigated. The catalytic activity is tabulated in Table 3 in terms of yield (%) and turn over frequency (TOF). The TOF values have been calculated based on the quaternary ammonium ions. No activity was observed either without the catalyst, MCM-41 (after calcination) and Cl-MCM-41 (Table 3, entry 1–2 and entry 5). This could be due to the lack of basic active sites in these catalysts. However, MCM-41 (before calcination) gave a conversion of 8.0% with selectivity of 49.0% towards SC. This result could be due to the presence of Br^- from CTAB which helps to attack SO to form a reactive intermediate [23]. According to the literature, about 88.4% styrene oxide was converted with 98.2% selectivity with the as-synthesized MCM-41 in 8 h [24]. It is postulated that, increasing the CTAB amount in the catalyst preparation method, elevate the conversion and selectivity of the products.

A higher selectivity of 97.0% with a TOF value of 13.2 h^{-1} was shown for MCM-41-Imi/Br in comparison with MCM-41-Imi (selectivity: 84.0%, TOF: 2.9 h^{-1}). This was achieved in 6 h run time with acetonitrile as solvent. Surprisingly, MCM-41-Imi/Br was also found to be very efficient under solvent-less condition. The highest catalytic activity for the solvent-less condition occured at 30 bar, 100 °C for 4 h and the result is shown in Table 3, entry 6. However, some traces of by-products such as styrene glycol was detected at the end of the reaction which was confirmed by GC–MS. The presence of by-product could be due to the interaction of water molecules trapped or adsorbed within the catalyst (silica matrix) which might promote the formation of the by-products. In order to explain the advantage of this study, the catalytic activity of MCM-41-Imi/Br was compared with similar RIm^+X^-MS-41 [22] and hybrid Ti(Al)-SBA-15 [23] catalysts. Both of these catalysts contain a functional organic (basic site) and a Lewis acid inorganic system which satisfy the requirements of an ionic liquid, but the catalyst preparation procedure remains complicated. In

Table 3
Reaction of styrene oxide (SO) with CO_2 using various heterogeneous catalysts[a].

Entry	Catalyst	Conversion (mol%)	Selectivity (mol%)	Yield[c] (mol%)	TOF[d]
1	Nil	–	–	–	–
2[b]	MCM-41 (after calcination)	–	–	–	–
3[b]	MCM-41 (before calcination)	8.0	49.0	3.9	0.7
4[b]	MCM-41-Imi	9.0	84.0	16.0	2.9
5[b]	Cl-MCM-41	–	–	–	–
6	MCM-41-Imi/Br	98.6	99.1	97.7	35.6
7[b]	MCM-41-Imi/Br	84.0	97.0	81.5	13.2

The by-product was the styrene glycols.
[a] Reaction conditions: SO = 3.5 mL (30 mmol), CO_2 = 30 bar, temperature = 100 °C, time = 4 h, catalyst amount = 200 mg, solvent = nil.
[b] Reaction conditions: SO = 3.5 mL (30 mmol), CO_2 = 40 bar, temperature = 140 °C, time = 6 h, catalyst amount = 300 mg, solvent = acetonitrile (50 mL).
[c] Yield (mol%) = conversion × selectivity, based on GC analysis.
[d] Turnover frequency: moles of styrene carbonate produced per mole of quaternary ammonium ion per hour.

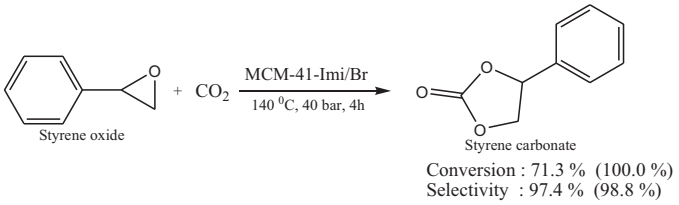

Scheme 2. The reaction of styrene oxide with carbon dioxide yielding styrene carbonate. (The value in parentheses is for solvent less reaction).

2006, Takahashi et al. [25] reported that silica supported phosphonium salt (SiO_2-[$PrBu_3P$]Br), showed higher reactivity (100% yield) for cyclic carbonate synthesis from propylene oxide (PO) and CO_2. The excellent performance was ascribed to the acidic surface silanol groups and the coordination of the group with a bromide ion to open the ring. In the current work, the MCM-41 material also plays an important role in enhancing the catalytic performance. At the same time, we found that, without the imidazole and 1,2-dibromoethane there is no synergistic effect in giving satisfactory catalytic activity. Further, the effect of temperature, CO_2 pressure, effect of reaction time, amount of catalyst and effect of solvent were investigated on MCM-41-Imi/Br. The general reaction scheme for the synthesis of styrene carbonate is shown in Scheme 2.

3.2.2. *Effect of reaction temperature*

The influence of temperature was tested over a broad temperature range from 80 to 160 °C on the conversion of styrene oxide. The data is shown in Fig. 5(a). The conversion increased progressively with an increase in reaction temperature up to 140 °C (96.6%). However, no further improvement in the conversion was noted at temperature greater than 140 °C. The selectivity of SC declined slightly when the reaction temperature was 160 °C. This was presumably due to the exothermic nature of the cycloaddition reaction which could lead to the polymerization of SC. Thus, 140 °C was found to be the optimal reaction temperature for this catalytic system. A similar temperature effect was reported by Jutz et al. [10] in the presence of Mn(salen)Br catalyst. They suggested that this behaviour was due to changes in phase distribution of the reactants at higher temperatures. However, such phenomenon was not observed with the MCM-41-Imi/Br system.

3.2.3. *Effect of CO_2 pressure*

The pressure of CO_2 has been known to be one of the most crucial factors affecting the cycloaddition reaction with epoxides. However, the pressure required to attain good catalytic activity is also dependent on the catalyst employed. In the cycloaddition reaction, CO_2 acts as both reactant and solvent [10]. For solvent and solventless reaction, an optimal ratio between SO and CO_2 of 1:20 and 1:16 was observed respectively. The effect of pressure was studied and the result is illustrated in Fig. 5(b). The conversion measured at a pressure of 20 bar was 83.4%. As the CO_2 increased to 40 bar and 60 bar progressively, the conversions increased to 95.8% and 99.0% respectively. However, the formation of by-products was observed at 60 bar. As could be seen from the curve, only ~50% conversion was obtained at a pressure of 80 bar. Thus, it could be concluded that increasing the CO_2 pressure results in a negative effect on the activity. A similar result was observed over betaine based salt catalyst [4]. This reduction could be due to the phase changes of CO_2 gas to super critical fluid. At this point, some of the SO can dissolve

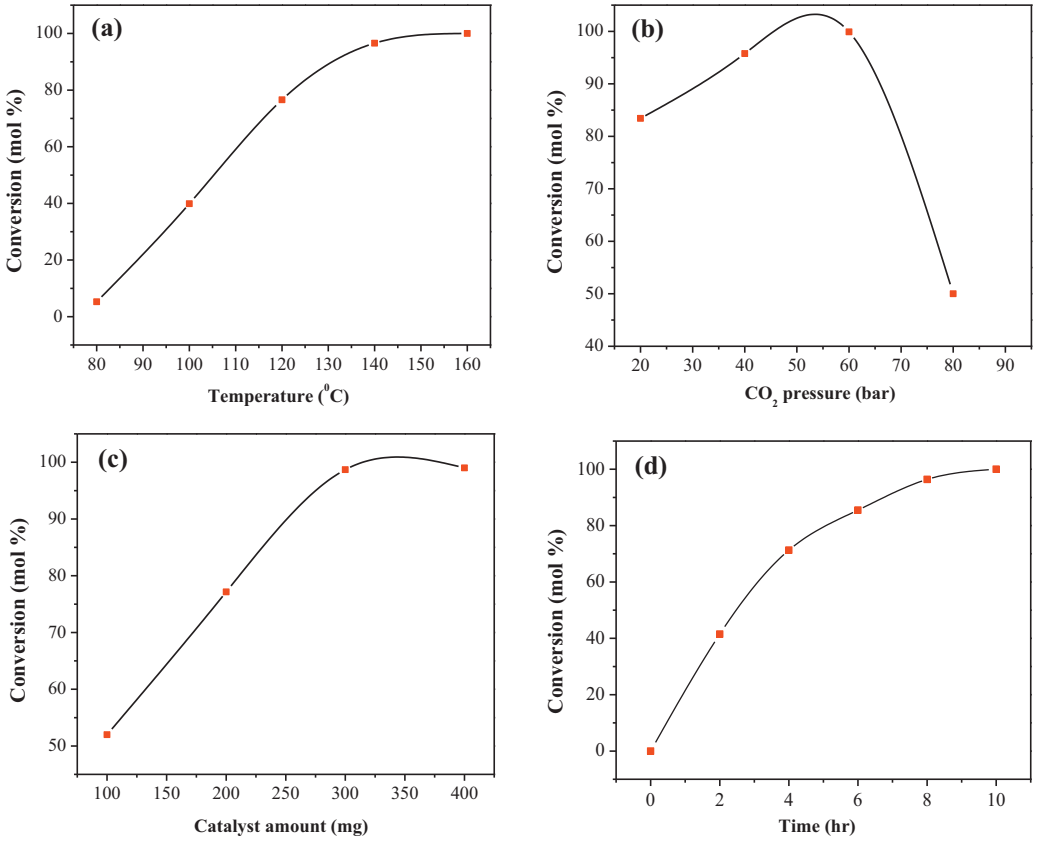

Fig. 5. The effects of different parameters on the conversion of the SO catalysed by MCM-41- Imi/Br carried out in acetonitrile as solvent. (a) The effect of reaction temperature, (reaction conditions: time = 8 h, pressure = 60 bar, catalyst weight = 300 mg), (b) the effect of pressure, (reaction conditions: time = 8 h, temperature = 140 °C, catalyst weight = 300 mg), (c) the effect of catalyst amount, (reaction condition: time = 8 h, temperature = 140 °C, pressure = 40 bar), (d) the effect of reaction time, (reaction conditions: temperature = 140 °C, pressure = 40 bar, catalyst weight = 300 mg). In all the cases, the amount of styrene oxide = 3.5 mL (30 mmol) and the solvent, acetonitrile = 50 mL.

Table 4
The effect of solvents on the cycloaddition reaction of CO_2 with styrene oxide.

Solvent	SO conversion (mol%)	Product selectivity (mol %)		TOF[a]
		SC	Others[b]	
None	100.0 (100.0)	93.6 (98.8)	6.4 (1.2)	15.1 (16.0)
Acetonitrile	85.5	97.0	3.0	13.5
N,*N*-dimethylformamide	71.5	97.6	2.4	11.3
Toluene	80.4	97.2	2.8	12.6
1,2-dichloroethane	35.5	88.3	11.7	5.1

Reaction conditions: catalyst = MCM-41-Imi/Br, time = 6 h, temperature = 140 °C, pressure = 40 bar, catalyst weight = 300 mg, SO = 3.5 mL (30 mmol).
The values in parentheses were obtained at 4 h with other variables fixed.
[a] Turnover frequency: moles of styrene carbonate produced per mole of quaternary ammonium ion per hour.
[b] The by-product were styrene glycols.

in the supercritical CO_2 which decreases the quantity of reactant available for reaction, which resulted in a reduced final yield.

3.2.4. Effect of catalyst amount

The amount of catalyst also influenced the performance of the reaction as shown in Fig. 5(c). A systematic study on the effect of catalyst mass was carried out ranging from 100 to 400 mg. It was found that 100 mg catalyst gave only 52% conversion. However, when the catalyst mass was increased by 2 folds, the conversion increased tremendously to 77.2%. The presence of more active sites at higher catalyst mass could lead to the observed conversion. A maximum conversion of 99.0% was attained when 300 mg catalyst was used. However, no further enhancement was noted when 400 mg was used. In fact a slight reduction in the selectivity was observed when the catalyst mass was 400 mg. Thus, it can be concluded that 300 mg was the optimal catalyst mass for the catalytic system studied.

3.2.5. Effect of reaction time

The influence of reaction time on the conversion was studied and the results are given in Fig. 5(d). At 6 h reaction time, 85.5% conversion was recorded. When the reaction time was prolonged to 8 h, a conversion of 96.4% was obtained. However, increasing the reaction time to 10 h did not affect the conversion, instead the formation of trace amount of by-products were noticed. It had taken a longer time of 8 h to obtain ca. 96% conversion (using acetonitrile as the solvent) because the SO is usually more difficult to convert to styrene carbonate due to the β-carbon atom being less reactive than other epoxides [26]. Thus, results showed that 8 h was needed to attain high conversion and selectivity. Therefore, the optimized conditions of this catalytic system are 140 °C, 40 bar of CO_2 pressure, 300 mg of MCM-41-Imi/Br and 8 h reaction time when acetonitrile was used as the solvent.

3.2.6. Effect of solvent

The effect of solvents on the cycloaddition reaction was investigated under the optimized reaction conditions. However, the reaction was only carried out for 6 h to save time. The results are tabulated in Table 4. The TOF value using different solvent increased in the following order: $C_2H_4Cl_2 < C_3H_7NO < C_6H_5CH_3 < CH_3CN <$ solvent-less. A polar aprotic acetonitrile, *N*,*N*-dimethylformamide (DMF) and non polar aprotic toluene gave almost similar conversion and selectivity. However, for 1,2-dichloroethane (a polar aprotic solvent), both conversion and selectivity were drastically reduced (conversion: 35.5%, selectivity: 88.3%). The decrease in activity might be attributed to the competitive adsorption of the more polar 1,2-dichloroethane solvent molecules on the active sites of the catalyst. As far as this study is concerned, acetonitrile was the most suitable solvent to transport the reactants to the reactive site of the catalyst to afford the corresponding cyclic carbonate. Aresta et al. [11] demonstrated that without catalyst, the use of DMF resulted in 34.7% yield of SC in 12 h at 50 bar and 135 °C. They suggested that, the amide group acted as a good promoter in the cycloaddition reaction.

Reactions without solvents are considered very desirable under the guidelines of Green Chemistry [1]. Surprisingly in this study, within 4 h, 100% conversion with 98.8% selectivity towards SC was observed under the solvent-less condition. This clearly indicates the interference of solvent molecules which can also adsorb on the active site, thereby resulting in low efficiency of the catalyst and a poor yield. This shows that the solvent-less condition and 4 h reaction time is optimal for this catalytic system.

3.2.7. Product identification and reusability of catalyst

The reaction mixture was diluted with acetonitrile and filtered to get a clear solution. On standing, the reaction mixture formed a yellow crystalline solid which was believed to be a mixture of styrene carbonate and styrene glycol. The crystal was crushed and mixed with silica gel which was then subjected to column chromatography. One of the fractions yielded a colourless crystalline solid which was identified by FT-IR, GC–MS and NMR spectroscopy. The following bands were found in the FT-IR (Nujol): 1812, 1779, 1358, 1169, 1054, 961, 759, and 698. These bands were consistent with that of SC which was confirmed by analyzing its GC–MS spectrum. The spectrum showed the molecular ion peak at m/z 164 $(M)^+$ which corresponds to $C_9H_8O_3$. Other fragments were at m/z 120, 105, 91, 90 (base peak), 78 and 65. ^{1}H NMR ($CDCl_3$, 500 MHz), δ (ppm): 7.36–7.48 (5H, m), 5.60–5.74 (1H, t), 4.78–4.86 (1H, t), 4.32–4.41 (1H, t). The FT-IR, GC–MS and ^{1}H NMR spectra are included in the supplementary data (Supplementary Figures 3–5).

The reusability of the catalyst is shown in Supplementary Figure 6. After each cycle, the catalyst was separated by filtration, washed with acetone and dried at 100 °C for 24 h before each reuse. The catalyst exhibited good stability and reusability. The slight decrease in the conversion could be due to the loss of bromide ions from the catalyst. However, the selectivity towards the SC remained constant (∼98.0%).

3.3. Characterization of reused catalyst

3.3.1. TEM analysis

The used catalyst was re-characterized in order to study the structural changes that might have occurred as a result of the catalytic activity. TEM analysis of the reused MCM-41-Imi/Br was carried out. The images are displayed in Supplementary Figure 7. The uniform hexagonal structure and straight channel along the (1 1 0) plane of MCM-41 support were clearly seen from the images. Hence, the highly ordered mesoporous structure of MCM-41-Imi/Br was still maintained even after several reuse. This confirmed the catalyst was thermally stable under the studied reaction conditions.

3.3.2. XRD analysis

The low angle XRD pattern of the reused catalyst is shown in the Supplementary Figure 8. The presence of peaks at $2\theta = 2.5$

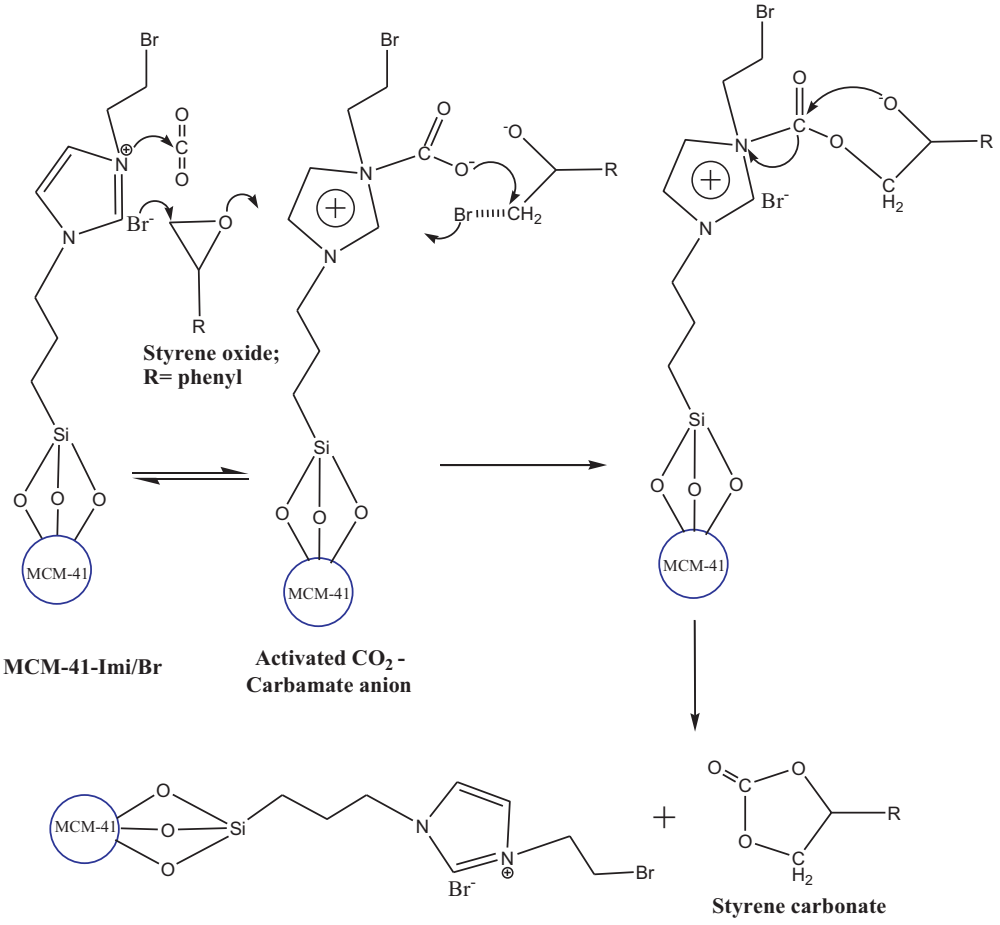

Scheme 3. The involvement of the halide (Br) and tertiary amine from MCM-41-Imi/Br on the ring opening of epoxide and activation of CO_2 in the reaction mechanism for the cycloaddition reaction.

corresponding to the (1 0 0) plane indicates that the ordering of the meso-structure does not change in the reused catalyst which suggests good structural stability.

3.3.3. *Ion chromatography analysis*

The ion chromatography analysis was conducted to determine the bromide ion composition in the reused catalyst. The loading of bromide in the reused MCM-41-Imi/Br was found to be 0.30 mmol/g. This value was very close to the fresh catalyst (0.44 mmol/g). The trivial disparity could be due to loss of active bromide during various cycle of reaction as expected. Nevertheless, it does not negate the conclusion of this study, i.e. the catalyst MCM-41-Imi/Br is stable and the active sites are not completely destroyed during the catalysis.

3.4. *Proposed reaction mechanism*

Based on the optimized reaction conditions, results and previously reported literature [22,24], a plausible reaction mechanism is suggested for the reaction between CO_2 and SO in the presence of MCM-41-Imi/Br as shown in Scheme 3.

First, the styrene oxide ring opens via nucleophilic (bromide) attack at the sterically less hindered β-carbon atom (—CH_2—) of the epoxide, generating an oxy anion. At the same time, CO_2 is activated by the tertiary amine from the catalyst. The attack of tertiary amine on CO_2 forms the carbamate anion. In the second step, the carbamate anion, attacks the (—CH_2—), and the bromide is detached from SO. Then oxygen from SO would attack the carbamate carbon which leaves the catalyst resulting in the formation of styrene carbonate.

In this catalytic system, the presence of a bromide ion and the tertiary nitrogen exhibit a synergistic effect to promote the reaction. As a comparison, in the case of MCM-41-supported guanidine

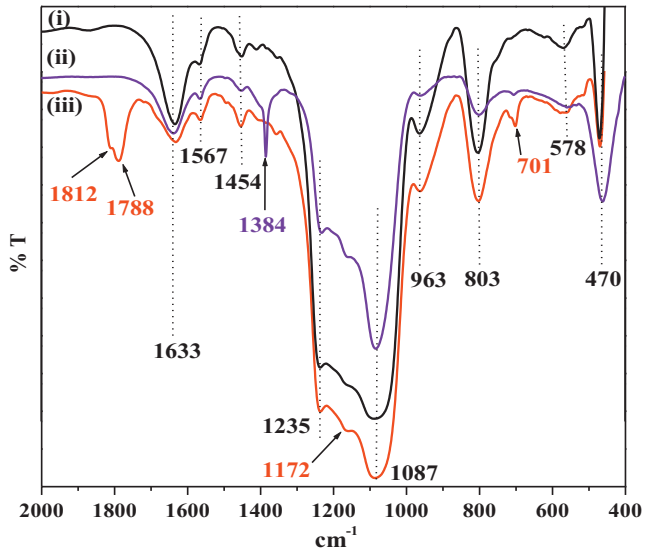

Fig. 6. The FT-IR spectra of the MCM-41-Imi/Br. (i) fresh catalyst, (ii) after the first reaction, (iii) adsorption of catalyst with CO_2.

catalysts, Barbarini et al. [3] suggested that the solid catalyst containing hydroxyl groups such as alcohol on the arm and silanols on the support surface could activate the epoxide by H-bond formation. On the other hand, they also observed that CO_2 was activated through the formation of the zwitterionic compound, which later add to the epoxide via nucleophilic attack. Obviously, in our work, the addition of 1,2-dibromoethane to the MCM-41-Imi, markedly improved the catalytic performance of MCM-41-Imi/Br.

To prove the reaction mechanism, the sites for CO_2 activation by the catalyst was investigated using FT-IR technique (Fig. 6). Several new transmission bands appeared in the catalyst after exposure to CO_2 under the optimum reaction condition. The band at 1812 and 1788 cm^{-1} are due to C═O and C—O bonds respectively. To further confirm the formation of carbamate anion, the FTIR of the used catalyst was compared with the FTIR of the fresh catalyst. The peak at 1384 cm^{-1} was due to C—O stretching vibration of the bidentate carbonate species and the peak at 1454 cm^{-1} corresponds to the symmetric C—O stretching vibration of the carbamate anion. Srivastava et al. [23] critically investigated the properties of their catalyst in the activation of CO_2. The CO_2 reacted with amine functional group in SBA-15-*pr*-Ade and Ti-SBA-15-*pr*-Ade showing the presence of the carbamate bands at 1609 and 1446 cm^{-1}.

4. Conclusion

In conclusion, the catalyst MCM-41-Imi/Br was successfully prepared and used in the cycloaddition reaction of CO_2 to styrene oxide. The amine and the bromide ion in the catalyst exhibit a synergistic effect to promote the reaction and this was the main reason for the high conversion and selectivity towards styrene carbonate. The catalyst was very effective under solvent-less conditions and without the need for co-catalysts. The catalyst was reused several times with only minor loss in the activity. The TEM and XRD analyses of the reused catalyst showed the preservation of the ordered hexagonal structures even after several consecutive cycles. This promises a truly heterogeneous, environmentally friendly and active catalyst for the production of cyclic carbonates from styrene oxide. A solvent less catalytic system certainly contribute to a better environment and green technology.

Acknowledgments

We would like to thank the Malaysian Government for a Research University Grant (Ac. No. 1001/PKIMIA/814127) and USM-RU-PRGS grant (1001/PKIMIA/844075) which partly supported this work. We would also like to thank the Malaysian Ministry of Higher Education for providing MyBrain15 Scholarship to JNA.

Appendix A. Supplementary data

Supplementary data associated with this article can be found, in the online version, at http://dx.doi.org/10.1016/j.apcatb.2013.01.049.

References

[1] R. Srivastava, D. Srinivas, P. Ratnasamy, Applied Catalysis A: General 289 (2005) 128–134.
[2] M. Alvaro, C. Baleizao, E. Carbonell, M.E. Ghoul, H. Garcia, B. Gigante, Tetrahedron 61 (2005) 12131–12139.
[3] A. Barbarini, R. Maggi, A. Mazzacani, G. Mori, G. Sartori, R. Sartorio, Tetrahedron Letters 44 (2003) 2931–2934.
[4] Y. Zhou, S. Hu, X. Ma, S. Liang, T. Jiang, B. Han, Journal of Molecular Catalysis A: Chemical 284 (2008) 52–57.
[5] M. Alvaro, C. Baleizao, D. Das, E. Carbonell, H. Garcia, Journal of Catalysis 228 (2004) 254–258.
[6] W.-L. Dai, L. Chen, S.-F. Yin, S.-L. Luo, C.-T. Au, Catalysis Letters 135 (2010) 295–304.
[7] M.M. Dharman, H.-J. Choi, S.-W. Park, D.-W. Park, Topics in Catalysis 53 (2010) 462–469.
[8] H. Kawanami, A. Sasaki, Y. Ikushima, http://www.isasf.net/fileadmin/files/Docs/Versailles/Papers/PRo4.pdf (accessed on the 5.04.12).
[9] A. Ghosh, P. Ramidi, S. Pulla, S.Z. Sullivan, S.L. Collom, Y. Gartia, P. Munshi, A.S. Biris, B.C. Noll, B.C. Berry, Catalysis Letters 137 (2010) 1–7.
[10] F. Jutz, J.-D. Grunwaldt, A. Baiker, Journal of Molecular Catalysis A: Chemical 279 (2008) 94–103.
[11] M. Aresta, A. Dibenedetto, L. Gianfrate, C. Pastore, Journal of Molecular Catalysis A: Chemical 204–205 (2003) 245–252.
[12] A. Sibaoih, P. Ryan, M. Leskela, B. Rieger, T. Repo, Applied Catalysis A: General 365 (2009) 194–198.
[13] B.M. Bhanage, S. Fujita, Y. Ikushima, M. Arai, Applied Catalysis A: General 219 (2001) 259–266.
[14] Malaysia Milled Rice Production Annual Growth Rate, [accessed 10.01.12] Available from World Wide Web http://www.indexmundi.com/agriculture/?country=my&commodity=milled-rice&graph=production-growth-rate
[15] F. Adam, R. Thankappan, Chemical Engineering Journal 160 (2010) 249–258.
[16] J.N. Appaturi, F. Adam, Z. Khanam, Microporous and Mesoporous Materials 156 (2012) 16–21.
[17] H. Yang, G.A. Ozin, C.T. Kresge, Advanced Materials 10 (1998) 883–887.
[18] F. Adam, S. Balakrishnan, P.-L. Wong, Journal of Physical Science 17 (2) (2006) 1–13.
[19] F. Adam, J.N. Appaturi, R. Thankappan, M.A.M. Nawi, Applied Surface Science 257 (2010) 811–816.
[20] F. Adam, K.M. Hello, H. Osman, Applied Catalysis A: General 382 (2010) 115–121.
[21] M.M. Rahman, M. Takafuji, H. Ihara, Journal of Chromatography A 1203 (2008) 59–66.
[22] S. Udayakumar, M.-K. Lee, H.-L. Shim, S.-W. Park, D.-W. Park, Catalysis Communications 10 (2009) 659–664.
[23] R. Srivastava, D. Srinivas, P. Ratnasamy, Microporous and Mesoporous Materials 90 (2006) 314–326.
[24] R. Srivastava, D. Srinivas, P. Ratnasamy, Tetrahedron Letters 47 (2006) 4213–4217.
[25] T. Takahashi, T. Watahiki, S. Kitazume, H. Yasuda, T. Sakakura, Chemical Communications 15 (2006) 1664–1666.
[26] K. Qiao, F. Ono, Q. Bao, D. Tomida, C. Yokoyama, Journal of Molecular Catalysis A: Chemical 303 (2009) 30–34.